EUROPEAN JOURNAL OF PURE AND APPLIED MATHEMATICS
Vol. 11, No. 4, 2018, 937-945
ISSN 1307-5543 – www.ejpam.com
Published by New York Business Global

Unsteady Stokes Flow through Porous Channel with Periodic Suction and Injection with Slip Conditions

Kaleemullah Bhatti[1], Zarqa Bano[1,*], Abdul Majeed Siddiqui[2]

[1] *Department of Mathematics and Social Sciences, Sukkur IBA University, Sukkur, Pakistan*
[2] *Department of Mathematics, Pennsylvania State University, York Campus, York, PA 17403, U.S.A.*

Abstract. This work is concerned with the influence of slip conditions on unsteady stokes flow between parallel porous plates with periodic suction and injection. The obtained unsteady governing equations are solved analytically by similarity method. The characteristics of complex axial velocity and complex radial velocity for different values of parameters are analyzed. Graphical results for slip parameter reveal that it has significant influence on the axial and radial velocity profiles. The effects of suction or injection are also observed. The problem of unsteady stokes flow through porous plates with no slip is recovered as a special case of our problem.

2010 Mathematics Subject Classifications: 76D05, 76D07

Key Words and Phrases: Unsteady Stokes Flow, Porous Plates, Periodic Suction and Injection, Wall Slip

---

1. Introduction

Unsteady Stokes flow of a Newtonian fluid in a channel is an interesting field due to its relevance to various engineering applications. Initially Berman A.S (1953) [1] studied the problem of unsteady laminar flow through porous walls. Ganesh [4] have recently applied similarity transformation method to solve problem of unsteady stokes flow through parallel porous plates when there is no slip between the fluid layer at the bottom and top and the corresponding walls. Kirubhashankar and Ganesh [2] then modified the problem by considering MHD fluid flow through the same channel of parallel porous plates. Unsteady incompressible MHD fluid flow through porous walls with slip conditions is studied recently by H. Zaman [3].

In this paper an analysis has been presented for the flow of a Newtonian fluid through a channel having parallel porous plates with periodic outward suction at upper wall and periodic injection of fluid through the lower wall. Also, we have considered the slippage

*Corresponding author.
DOI: https://doi.org/10.29020/nybg.ejpam.v11i4.3309

Email addresses: zarqa.bano@iba-suk.edu.pk (Z. Bano), kaleem.msmts@iba-suk.edu.pk (K. Bhatti)

effect of fluid layer connected to the plates. An exact solution to Navier Stokes equations, reduced to forth order linear ordinary differential equation with the slip boundary conditions is obtained. The similarity transformation method is adopted to solve the dynamic equations for small flow through porous plates. Ganesh's work [4] can be considered as a special case of our work when no slip occurs.

2. Main Problem

2.1. Problem Formulation

Two infinite porous parallel plates are considered at **y**=0 and **y**=H. An incompressible Newtonian fluid flows through these fixed flat plates. We assume the Stokes flow and there is a periodic injection with velocity $\mathbf{V_1 e^{i\omega t}}$ at lower plate and a periodic suction with velocity $\mathbf{V_2 e^{i\omega t}}$ at upper plate. In addition we consider slip between the fluid layer in contact with the wall according to Navier slip law which states that the relative velocity of the fluid and the wall is proportional to the shear rate at the wall.
Let u and v be the components of velocity vector in **x** and **y** direction in flow field at any time t. We chose velocity vector $\vec{\mathbf{q}}$ and pressure P in the form:

$$\vec{\mathbf{q}} = \left\{ u(x,y)\hat{i} + v(x,y)\hat{j} \right\} e^{i\omega t}, \tag{1}$$

$$P = p(x,y)e^{i\omega t}, \tag{2}$$

Under the above assumptions and the choice of rectangular co-ordinate system the governing equations are:

$$\frac{\partial u}{\partial x} + \frac{\partial v}{\partial y} = 0, \tag{3}$$

$$\rho\frac{\partial u}{\partial t} = -\frac{\partial p}{\partial x} + \mu(\frac{\partial^2 u}{\partial x^2} + \frac{\partial^2 u}{\partial y^2}), \tag{4}$$

and

$$\rho\frac{\partial v}{\partial t} = -\frac{\partial p}{\partial y} + \mu(\frac{\partial^2 v}{\partial x^2} + \frac{\partial^2 v}{\partial y^2}), \tag{5}$$

where μ is the co-efficient of viscosity and ρ is constant density of the fluid. The convective terms in the governing equations are neglected due to very small Reynolds number. The boundary conditions of the problem are:

$$u(x,0) = \lambda \left| \frac{\partial u}{\partial y} \right|_{y=0}, \tag{6}$$

$$u(x,H) = \lambda \left| \frac{\partial u}{\partial y} \right|_{y=H}, \tag{7}$$

and

$$v(x,0) = V_1, \quad v(x,H) = V_2. \tag{8}$$

2.2. Analytical Solution

For a two dimensional incompressible flow a stream function ψ is introduced for which,

$$u(x,y) = \frac{\partial\psi}{\partial y} \quad v(x,y) = -\frac{\partial\psi}{\partial x}, \tag{9}$$

such that the continuity equation (3) is automatically satisfied. Using (1), (2) and (9) in Equations (4) and (5) we get,

$$\rho i\omega \frac{\partial\psi}{\partial y} = -\frac{\partial p}{\partial x} + \mu \frac{\partial}{\partial y}\left(\nabla^2\psi\right), \tag{10}$$

and

$$\rho i\omega \frac{\partial\psi}{\partial x} = \frac{\partial p}{\partial y} + \mu \frac{\partial}{\partial x}\left(\nabla^2\psi\right). \tag{11}$$

For the constant wall velocity $v_w = 0$ and given BC's, a suitable choice of stream function is,

$$\psi(x,y) = \left(H\frac{u_0}{a} - v_2 x\right) f(\eta), \tag{12}$$

where u_0 is the average entrance velocity. $a = 1 - v_1/v_2$, with $1 \lessapprox |v_1| \lessapprox |v_2|$ and $\eta = y/h$ is called dimensionless distance. Using equation (12) in equations (10) and (11) we get,

$$-\frac{1}{\rho}\frac{\partial p}{\partial x} = \left(\frac{u_0}{a} - \frac{v_2 x}{H}\right)\left[i\omega f'(\eta) - \frac{\nu}{H^2} f'''(\eta)\right], \tag{13}$$

and

$$-\frac{1}{\rho H}\frac{\partial p}{\partial \eta} = i\omega v_2 f(\eta) - \frac{\nu}{H^2} v_2 f''(\eta). \tag{14}$$

Differentiating (13) with respect to η and (14) with respect to x we get,

$$-\frac{1}{\rho}\frac{\partial^2 p}{\partial\eta\partial x} = \left(\frac{u_0}{a} - \frac{v_2 x}{H}\right)\left[i\omega f''(\eta) - \frac{\nu}{H^2} f^{(iv)}(\eta)\right], \tag{15}$$

and

$$\frac{\partial^2 p}{\partial x\partial\eta} = 0. \tag{16}$$

Comparing (15) and (16) we get,

$$f^{(iv)}(\eta) - \frac{i\omega H^2\rho}{\mu} f''(\eta) = 0. \tag{17}$$

Assuming $\alpha^2 = \frac{i\omega\rho}{\mu}$, (17) reduces to the form,

$$f^{(iv)}(\eta) - \alpha^2 H^2 f''(\eta) = 0. \tag{18}$$

Also using stream function defined by (9) and (12) and the slip boundary conditions (6)to (8), we get following new boundary conditions on $f(\eta)$,

$$hf'(0) = \lambda f''(0), \tag{19}$$

$$hf'(1) = \lambda f''(1), \tag{20}$$

$$f(0) = 1 - a, \tag{21}$$

and

$$f(1) = 1. \tag{22}$$

Solving (18) subjected to the above boundary conditions to get $f(\eta)$ and then using this accompanied with (1) and (9) we get,

$$u = u(x, y)e^{i\omega t},$$

$$u = \frac{\partial \psi}{\partial y} e^{i\omega t},$$

$$u = \left(\frac{u_0}{a} - \frac{v_2 x}{H}\right) f'(\eta) e^{i\omega t},$$

$$\begin{aligned} u \;=\; & H\alpha a \left(\frac{u_0}{a} - \frac{v_2 x}{H}\right) [\frac{\alpha\lambda(\alpha\lambda \sinh \alpha H + \cosh \alpha y - \cosh \alpha(H - y))}{\alpha^3 H\lambda^2 \sinh \alpha H - \alpha H \sinh \alpha H + 2\cosh \alpha H - 2} \\ & + \frac{\sinh \alpha(H - y) + \sinh \alpha y - \sinh \alpha H}{\alpha^3 H\lambda^2 \sinh \alpha H - \alpha H \sinh \alpha H + 2\cosh \alpha H - 2}] e^{i\omega t}, \end{aligned} \tag{23}$$

and

$$v = v(x, y)e^{i\omega t},$$

$$v = -\frac{\partial \psi}{\partial x} e^{i\omega t},$$

$$\begin{aligned} v \;=\; & v_2[\frac{a\alpha(\lambda \sinh \alpha y + \lambda \sinh \alpha(H - y) - y \sinh \alpha H + H \sinh \alpha H - \lambda \cosh \alpha H)}{\alpha^3 H\lambda^2 \sinh \alpha H - \alpha H \sinh \alpha H + 2\cosh \alpha H - 2} \\ & + \frac{a(\cosh \alpha y - \cosh \alpha H - \cosh \alpha(H - y) - H \sinh \alpha H + 1)}{\alpha^3 H\lambda^2 \sinh \alpha H - \alpha H \sinh \alpha H + 2\cosh \alpha H - 2} \\ & + \frac{\alpha^3\lambda^2(H - aH + ay) \sinh \alpha H + 2(\cosh \alpha H - 1)}{\alpha^3 H\lambda^2 \sinh \alpha H - \alpha H \sinh \alpha H + 2\cosh \alpha H - 2}] e^{i\omega t} \end{aligned} \tag{24}$$

As a special case we present here the expression for velocity profile obtained by for λ=0.

$$u = H\alpha a \left(\frac{u_0}{a} - \frac{v_2 x}{H}\right) [\frac{\sinh \alpha(H - y) + \sinh \alpha y - \sinh \alpha H}{-\alpha H \sinh \alpha H + 2\cosh \alpha H - 2}] e^{i\omega t}, \tag{25}$$

and

$$v = v_2 \frac{\alpha(aH - ay - H) \sinh \alpha H + (2 - a)\cosh \alpha H + a(\cosh \alpha y - \cosh \alpha(H - y)) - 2}{-\alpha H \sinh \alpha H + 2\cosh \alpha H - 2} e^{i\omega t} \tag{26}$$

Equation (25) and (26) match with the axial and radial velocity profiles in [4].

2.3. Pressure Distribution

The pressure distribution can be obtained by extracting the pressure gradients from (13) and (14) and then by integrating with respect to x and η respectively. Thus

$$\int_0^x \frac{\partial p}{\partial x} dx = p(x,\eta) - p(0,\eta) \tag{27}$$

$$\int_0^\eta \frac{\partial p}{\partial \eta} d\eta = p(x,\eta) - p(x,0) \tag{28}$$

Now it follows from (27) and (28) that

$$\int_0^x \frac{\partial p}{\partial x} dx + \left(\int_0^\eta \frac{\partial p}{\partial \eta} d\eta \right)_{x=0} = p(x,\eta) - p(0,0) \tag{29}$$

Using (13) and (14) we get,

$$p(x,\eta) = p(0,0) + \frac{\rho v_2}{2H}\left(iwf(\eta) - \frac{\nu f'''(\eta)}{H^2} \right) x^2 - \frac{\rho u_0}{a}\left(iwf(\eta) - \frac{\nu f'''(\eta)}{H^2} \right) x$$
$$- \frac{\rho v_2}{H}\left(\int_0^\eta (H^2 iwf(\eta) - \nu f''(\eta)) d\eta \right) \tag{30}$$

Where p(0,0) is pressure at the entrance of the channel.

2.4. Results and Discussion

The numerical values of axial and radial velocity components have been calculated for different values x, ωt and slip parameter λ.

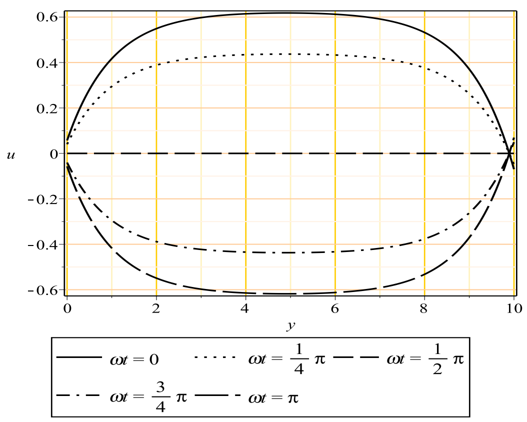

Figure 1: Axial velocity profile for λ=0.1, $v_1 = 1$, $v_2 = 2$ $x = 0$, $H = 10$, $u_0 = 0.5$ and α=1 for different values of ωt

Figures 1 to 7 are axial velocity profiles at different cross sections of the channel namely at $x = 0$, $x = 2$ and $x = 4$ and for different values of slip parameter namely for $\lambda = 0$,

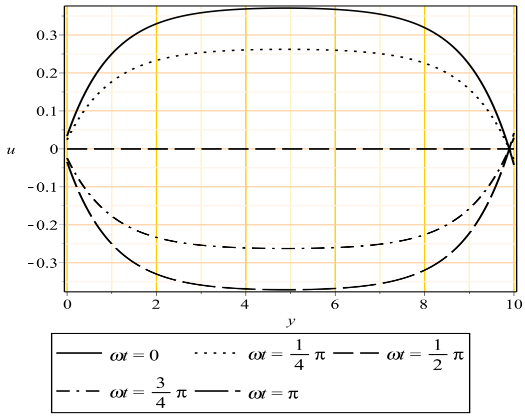

Figure 2: Axial velocity profile for λ=0.1, $v_1 = 1$, $v_2 = 2$ $x = 2$, $H = 10$, $u_0 = 0.5$ and α=1 for different values of ωt

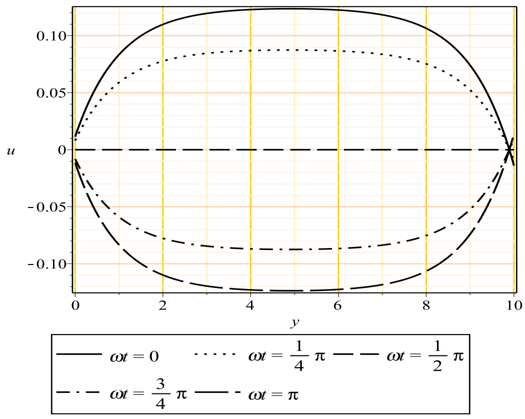

Figure 3: Axial velocity profile for λ=0.1, $v_1 = 1$, $v_2 = 2$ $x = 4$, $H = 10$, $u_0 = 0.5$ and α=1 for different values of ωt

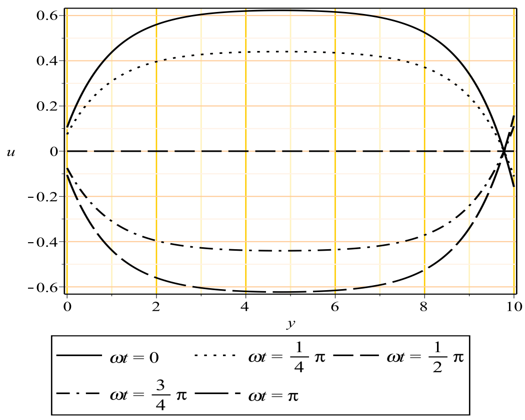

Figure 4: Axial velocity profile for λ=0.2, $v_1 = 1$, $v_2 = 2$ $x = 0$, $H = 10$, $u_0 = 0.5$ and α=1 for different values of ωt

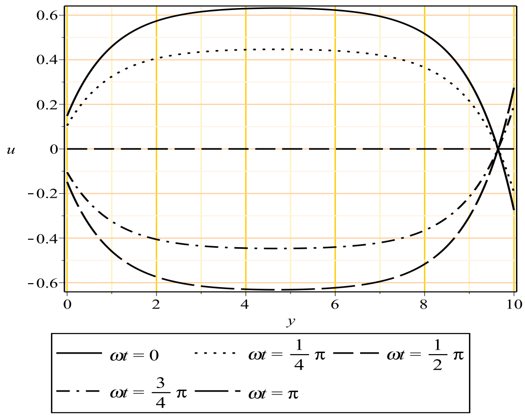

Figure 5: Axial velocity profile for λ=0.3, $v_1 = 1$, $v_2 = 2$ $x = 0$, $H = 10$, $u_0 = 0.5$ and α=1 for different values of ωt

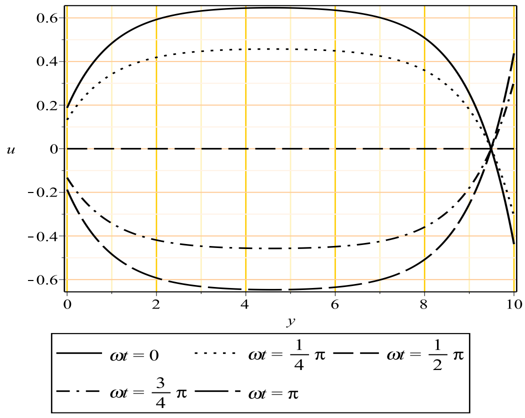

Figure 6: Axial velocity profile for λ=0.4, $v_1 = 1$, $v_2 = 2$ $x = 0$, $H = 10$, $u_0 = 0.5$ and α=1 for different values of ωt

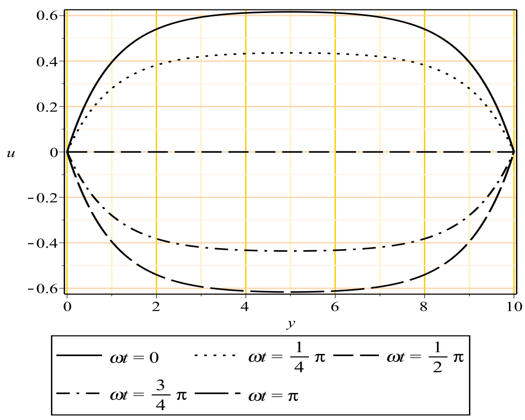

Figure 7: Axial velocity profile for λ=0, $v_1 = 1$, $v_2 = 2$ $x = 0$, $H = 10$, $u_0 = 0.5$ and α=1 for different values of ωt

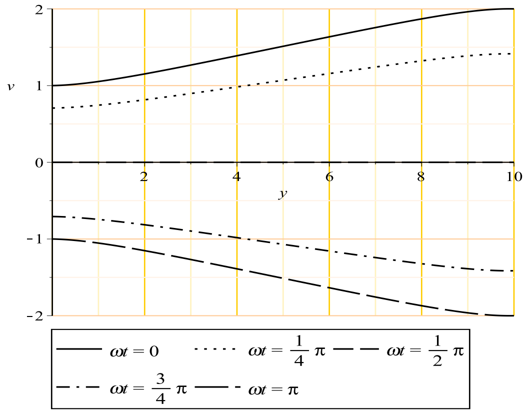

Figure 8: Radial velocity profile for λ=0.1, $v_1 = 1$, $v_2 = 2$, $H = 10$ and α=1 for different values of ωt

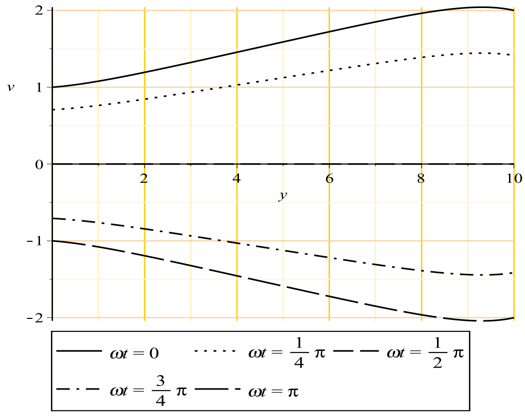

Figure 9: Radial velocity profile for λ=0.5, $v_1 = 1$, $v_2 = 2$, $H = 10$ and α=1 for different values of ωt

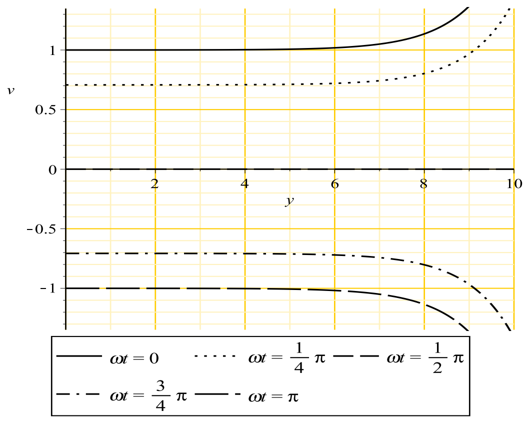

Figure 10: Radial velocity profile for λ=1, $v_1 = 1$, $v_2 = 2$, $H = 10$ and α=1 for different values of ωt

$\lambda = 0.1$, $\lambda = 0.2$ and $\lambda = 0.3$ and $\lambda = 0.4$, when average entrance velocity is $u_0 = 0.5$. It is observed from Figure 1, 2 and 3 that the magnitude of axial velocity decreases as x increases from 0 to 4. The same result is obtained by Ganesh [4] for no slip problem. Figures 1, 4, 5, 6 and 7 show the effect of slip parameter λ. It is clearly seen that as λ increases from 0 to 0.4 the magnitude of axial velocity near the plates at $y = 0$ and $y = 10$ also increases. Figure 8, 9 and 10 depict the radial velocity profile for $v_1 = 1$, $v_2 = 2$ and $\alpha = 1$, for different values of ωt. It is very clear that the radial velocity completely vanishes for $\omega t = \frac{\pi}{2}$ and it is non-linear for other values of ωt. It is also seen that when slip parameter increases from $\lambda = 0$ to $\lambda = 1$, the magnitude of radial velocity decreases and behaves nearly like a constant.

2.5. Conclusion

In the above analysis, an exact solution for velocity field of unsteady stokes flow of viscous fluid between two parallel plates in the presence of porous walls and slippage effects is constructed. The graphical analysis has been made for different values of the slip parameter at various cross sections of the channel. The expressions of axial and radial velocities which are presented here reduce to the Ganesh's results for the case when there is no slip at wall. We presume that the results obtained here add one more class of exact solution to that of a few presently available in the literature.

References

[1] Abraham S. Berman. Laminar flow in channels with porous walls. *Journal of Applied Physics*, 24(9):1232–1235, 1953.

[2] Dr. S. Ganesh C. K. Kirubhashankar and A. Mohamed Ismail. An Exact Solution of The Problem Of Unsteady MHD Flow Through Parralel Porous Plates. *Int'l Journal of Advances in Mechanical Automobile Engg.*, 1:39–42, 2014.

[3] H.Zaman. Hall Effects on The Unsteady Incompressible MHD Fluid Flow With Slip Conditions And Porous Walls. *Applied Mathematics and Physics*, 1(2):31–38, 2013.

[4] Ganesh S and Krishnambal S. Unsteady Stokes Flow Of Viscous Fluid Between Two Parallel Porous Plates. *Journal on Information Sciences and Computing*, 1(1):63–66, 2007.